DOI: 10.1021/ma1000783

Macromolecules
ARTICLE

Synthesis and Thermo-/pH- Dual Responsive Properties of Poly(amidoamine) Dendronized Poly(2-hydroxyethyl) Methacrylate

Min Gao,[†] Xinru Jia,*[,†] Yan Li,[†] Dehai Liang,[†] and Yen Wei[‡]

[†]*Beijing National Laboratory for Molecular Sciences, Key Laboratory of Polymer Chemistry and Physics of the Ministry of Education, College of Chemistry and Molecular Engineering, Peking University, Beijing 100871 China, and* [‡]*Department of Chemistry, Tsinghua University, Beijing 100084, China*

Received January 12, 2010; Revised Manuscript Received April 2, 2010

ABSTRACT: The first and second generation poly(amidoamine) dendronized poly(2-hydroxylethyl) methacrylate (**PG*n*-macro** (n = 1, 2)) were synthesized by the macromonomer approach. The structures and molecular weights of the obtained polymers were characterized by ^{1}H NMR, FTIR, and GPC. UV−vis turbidity measurements revealed that all the resultant polymers were thermo-responsive, exhibiting the LCSTs in the range of 16−33 °C. The polymers also showed pH sensitive for the existence of the tertiary amino groups in the interior of the pendent dendrons. It was found that the generation of the dendrons, the molecular weights of the polymers, the concentrations, and the pHs showed great influence on the lower critical solution temperatures (LCSTs) of the polymer solutions. The higher LCST could be achieved either by increasing the generation of the dendrons or by decreasing the molecular weight. The dilute polymer solution with lower pH displayed the higher LCST. For example, the LCST of **PG1-macro** solution increased significantly with the pH decreased below 7.0, but the decrease of LCST was much slower at pH ≥ 7.0. DLS experiments at variable temperatures demonstrated that the polymer chains spontaneously aggregated to form large size particles as increasing the temperature above LCST due to the dehydration of the peripheral butylamide groups and the enhanced hydrophobic interactions. The morphology of aggregates was directly visualized by optical microscopy, and uniform spherical aggregates with the diameter of 3−7 μm were observed.

Introduction

As stimuli-responsive behavior is a typical feature of biomaterials, developing stimuli-responsive polymers, especially polymers with dual- or multiresponsive properties,[1−6] remains a challenge. They have drawn an increasing attention due to their potential applications in many fields, such as drug delivery, gene carriers, sensors, catalysis, and chromatography separation.[7−12] Up to now, most of the synthesized stimuli-responsive polymers and copolymers are classified as linear structures and their responsiveness mainly derives from the function of monomers or the structural arrangement of the macromolecules as to the variation of environmental conditions. For example, the ratio of hydrophilic and hydrophobic units may dominate the thermo-responsiveness of the polymers.[13,14] The ionizable moieties create the polymers with pH-responsiveness.[15] Notably, it has been reported recently that not only the responsive units endow the polymers with environmental sensitivity, but also the location, the special distribution of these units, and the molecular shape impact the responsiveness greatly. Such an architecture effect may generate the polymers with unpredictable properties. For example, Kono et al. reported that the lower critical solution temperature (LCST) of isobutyramide (IBAM) shelled poly(amidoamine) (PAMAM) and poly(propylenimine) (PPI) dendrimers showed more remarkable molecular weight dependence,[16] and the heat of phase transition of the NIPAM-terminated G4.5 or G5 PAMAM dendrimers was extremely small as compared to the linear PNIPAM, suggesting that the structural features of dendrimers played a crucial role in determining the thermo-responsive properties.[17]

Dendronized polymers, a merger of two concepts of dendrimers and polymers, possess the particular structures constructed by a linear polymer backbone surrounded with certain structural dendrons at each repeating unit.[18] Such polymers may maintain the flexibility of the linear polymer chains with lower generation dendrons as the side groups, and they may display a rigid, cylindrical shape by attaching higher generation dendritic side chains. Dendronized polymers could be prepared via three general synthetic strategies, including the graft-to, the graft-from, and the macromonomer approaches.[19] One obvious advantage of "the macromonomer approach" over the other two methods lies in that the obtained polymers exhibit a quantitative degree of dendron attachment, which can be defined as "structurally perfect" comb polymers. Over the last 20 years, many efforts have been paid on modifying dendronized polymers with various functions. Fréchet et al.[20] prepared a pyrrolidinopyridine embedded dendronized cyclocopolymer through divergent growth techniques. They found that the microenvironment created by the polyester-type dendrons could be used to catalyze the difficult esterification of a tertiary alcohol with pivalic anhydride. Peng et al.[21] synthesized a series of polyfluorenes dendronized with functional carbazole and oxazole side chains. Because of less aggregation of the main chains with the steric hindrance of dendritic units, the photoluminescent (PL) and electroluminescent (EL) emission color quality was highly improved. These copolymers were promising candidates for both efficient pure blue emitters and host materials for highly efficient phosphorescent PLEDs. Attractively, dendronized polymers with stimuli-responsive properties have been explored. The advantages of such polymers with stimuli-responsiveness refer to that the responsive motifs can be easily incorporated into the polymers for the densely packed modifiable peripheral groups of dendrons; the balance of the molecular structures, for example, the hydrophilicity−hydrophobicity ratios can be easily tuned by converting the generation, interior building blocks, and surface groups of the dendrons; and the unique architecture may lead to

*Corresponding author. Telephone: +86 10 62752102. Fax: +86 10 62751708. E-mail: xrjia@pku.edu.cn.

 Published on Web 04/16/2010 © 2010 American Chemical Society

Scheme 1. Synthesis and Structures of Dendritic Monomers G*n*-macro and the Corresponding Dendronized Polymers PG*n*-macro (*n* = 1, 2)

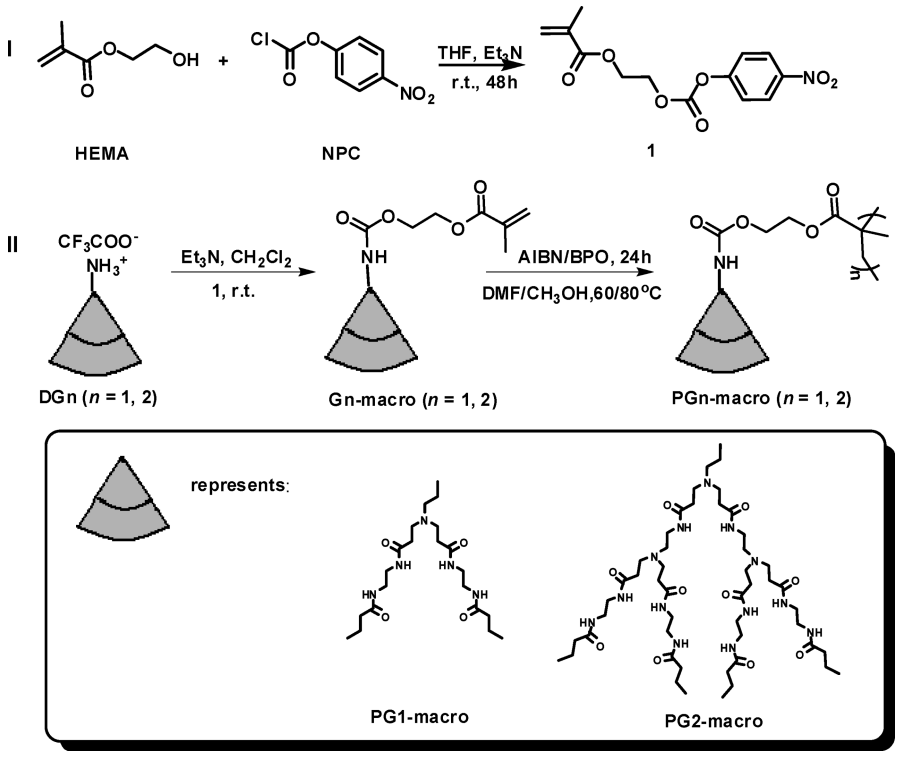

fast and sharp transitions. Zhang et al. synthesized a series of the first and second generation dendronized polymethacrylate derivatives using gallic acid as branching point and oligoethylene glycol (OEG) units as the linker. All these polymers exhibited sharp phase transitions with negligible hystereses in the aqueous solution with LCST values in the range of 33−65 °C.[22,23] Further study by Ballauff and Zhang et al. demonstrated that stable and monodisperse mesoglobules were formed by the second generation dendronized polymer (PG2) at the temperatures higher than 35 °C (LCST). Interestingly, these globules could completely dissociate back upon cooling without hysteresis.[24] Very recently, Zhang and co-workers[25] successfully synthesized the OEG-based third generation dendronized polymer (PG3) with a polymerization degree of 16 determined by GPC. As the lower generation counterparts,[22,23] PG3 also showed a fast and sharp phase transition with an apparent LCST of 34 °C in the aqueous solution.

However, dendronized polymers with stimuli-responsive properties have not been reported extensively and those with thermo- and pH- dual responsive behavior are still rare. In our previous study,[26] we reported the synthesis of thermo- and pH- dual responsive dendronized polymers (**PSADG1**−**PSADG3**) by attaching butylamide terminated poly(amidoamine) dendrons (**DG1**−**DG3**) to the alternating copolymers of styrene and maleic anhydride. The LCSTs of the resulting polymers could be tuned by changing generation and coverage degree of the dendrons, by altering the concentration of the polymers, and also by adding salt and changing pH of the solutions. However, due to the deficiency of the graft-to route, the structures of these dendronized polymers were not defined or well controlled. Herein, we report a new kind of thermo- and pH- dual responsive dendronized polymers (**PG*n*-macro** (*n* = 1, 2)) composed of a linear poly(2-hydroxyethyl) methacrylate pendant with butylamide terminated poly(amidoamine) dendrons (**DG1**−**DG2**) at each repeating unit. The polymers were synthesized by the macromonomer route as shown in Scheme 1. The structures, molecular weights, thermal properties, thermo- and pH-dual responsive properties were studied by ^{1}H NMR, FTIR, GPC, DSC, UV−vis, laser light scattering (LLS), and optical microscopy (OM). All the obtained dendronized polymers were thermoresponsive and pH-sensitive in 10 mM phosphate buffer. The LCSTs of the polymers were dependent on the generation of the dendrons, the molecular weights of the polymers, the concentration, and the pH of the solutions. These polymers spontaneously formed larger aggregates that scattered light efficiently upon heating above LCST.

Experimental Section

Materials. Poly(amidoamine) dendrons **DG*n*** (*n* = 1−2) (Scheme 1) were synthesized according to the method reported previously.[27] *N*,*N*-dimethylformamide, triethylamine, dichloromethane, tetrahydrofuran, 2,2′-azobis(isobutyronitrile) (AIBN), and benzoyl peroxide (BPO) were purified according to the standard procedures. Unless stated otherwise, all the reagents and the common solvents were obtained from commercial sources and used as received.

Measurements. ^{1}H NMR and ^{13}C NMR spectra were recorded on 300 MHz (Varian Mercury) or 400 MHz (Bruker) spectrometers operated at room temperature, with $CDCl_3$ or DMSO-d_6 as the solvents and tetramethylsilane (TMS) as the internal standard. FTIR spectra were obtained on a VECTOR 22 Fourier transform IR spectrometer (Bruker). The electrospray ionization mass spectra (ESI MS) were obtained using a APEX IV Fourier transform ion cyclotron resonance mass spectrometer (Bruker). For UV−vis turbidity measurements, the LCSTs were determined on a Varian CARY 1E UV−vis spectrophotometer, equipped with a BECKMAN 9112AA2E (PolyScience) thermostatic bath. The heating rate was about 0.5 °C/min. The temperature of the phase transition (LCST) was defined as the one at which the transmittance at λ = 550 nm had reached 50% of its initial value. Through the turbidity measurements, the pH_{tran} values were also obtained by determining a series of polymer solutions (0.25 mg mL^{-1}) with different pHs at 25 °C. The pH_{tran} was defined as the pH at which the transmittance at λ = 550 nm had reached 50% of its initial value (the transmittance at low pH). A gel permeation chromatograph (GPC) equipped with a Waters 2410 refractive-index detector, a Waters 515 HPLC pump, and

Waters styragel columns (HT3 and HT4) with DMF containing 0.05 wt % LiBr as an eluent at a flow rate of 1.0 mL/min. Monodispersity polystyrene standards were used for calibration. Differential scanning calorimetry (DSC) measurements were carried out on TA Instruments DSC Q100. Polymer samples were sealed in aluminum pans. An empty aluminum pan was used as the reference. A scanning rate of 10.0 °C/min was used for both heating and cooling processes between −10 and +180 °C. The glass transition temperature (T_g) was obtained from the first cooling run and corresponded to the midpoint of discontinuity in the heat flow. The dynamic light scattering (DLS) experiments of **PG1-macro** at 0.25 mg mL^{-1} in 10 mM phosphate buffered solution at different pHs were performed on a Brookhaven goniometer (BI-200SM) equipped with a BI-TurboCorr digital correlator and a thermostatic bath with temperature accuracy of 0.01 °C. A vertically polarized solid-state laser operating at 532 nm was used as the light source (100 mW, CNI Changchun GXC-III, China). The stock solutions were filtered through a Millipore 0.45 μm PVDF filter into a dust-free vial. During heating, the autocorrelation functions were collected when the scattered intensity at each temperature became stable. The time correlation functions were analyzed with a Laplace inversion program CONTIN. Optical microscopy images of polymer solutions were recorded using a Leica DLMP microscope. The polymer solution was placed on a glass slide and the sample was heated from room temperature (ca. 18 °C) to 40 °C with the heating rate of 2 °C/min. The micrographs were recorded by a Digital sight camera at a specific temperature in the process.

Synthesis of Monomer G1-macro. Here, 0.39 g (3.0 mmol) of 2-hydroxyethyl methacrylate (HEMA) and 0.36 g (3.6 mmol) of triethylamine (TEA) were dissolved in 12 mL of anhydrous THF. Then a THF solution of 0.71 g (3.5 mmol) of 4-nitrophenyl chloroformate was added in an ice bath. After the solution was stirred at room temperature for 48 h, the produced white salt TEA·HCl was filtrated, and the filtrate was collected and evaporated in vacuo. The middle product 2-((4-nitrophenoxy)carbonyloxy)ethyl methacrylate (**1**, Scheme 1) was used without further purification and its structure was proved by ^{1}H NMR spectrum (Figure S1, Supporting Information). Then, a dichloromethane solution of **1** was added dropwise to an ice-cooled, stirred solution of 0.91 g (1.7 mmol) of **DG1** and 0.35 g (3.5 mmol) of TEA in dry CH_2Cl_2 (15 mL). The mixture was stirred at room temperature for 48 h and the solvent was evaporated in vacuo. The crude product was purified first by dissolution−precipitation repeatedly from chloroform/diethyl ether (1/20) and then through a short silica column quickly to afford the monomer **G1-macro** as a pale yellow solid with 78.6% yield (0.77 g). The structure and molecular weight of the monomer were determined by ^{1}H NMR, ^{13}C NMR, FTIR, and ESI MS.

G1-macro. This was obtained as a pale yellow solid. Yield: 78.6%. ^{1}H NMR (300 MHz, $CDCl_3$, TMS, T = 298 K): 7.65−7.40 (br, 2H, CON*H*), 6.90−6.72 (br, 2H, CON*H*), 6.13 (s, 1H, C*H*$_2$=C), 6.05−5.80 (m, 1H, OCON*H*), 5.61−5.60 (t, 1H, C*H*$_2$=C), 4.46−4.20 (m, 4H, OC*H*$_2$C*H*$_2$O), 3.35 (s, 8H, NHC*H*$_2$C*H*$_2$NH), 3.30−3.20 (m, 2H, C*H*$_2$CH$_2$N), 2.68 (t, 4H, C*H*$_2$CH$_2$CO), 2.52 (t, 2H, CH$_2$C*H*$_2$N), 2.36−2.34 (t, 4H, CH$_2$C*H*$_2$CO), 2.19−2.14 (t, 4H, C*H*$_2$CH$_2$CH$_3$), 1.92 (s, 3H, CH$_2$=C(C*H*$_3$)), 1.70−1.60 (m, 4H, CH$_2$C*H*$_2$CH$_3$), 0.96−0.91 (t, 6H, CH$_2$CH$_2$C*H*$_3$). ^{13}C NMR (75 MHz, $CDCl_3$, TMS, T = 298 K): 174.38, 174.22, 167.14, 156.33, 135.80, 126.00, 62.76, 62.39, 52.57, 50.00, 39.39, 39.23, 38.51, 38.25, 33.42, 18.97, 18.10, 13.60. FTIR (KBr, cm^{-1}): 3300 (br), 3087, 2962, 2874, 1715, 1647, 1546, 1452, 1377, 1251, 1161, 1046, 946, 691. ESI MS: calcd for $C_{27}H_{48}N_6O_8$, 584; found, 585 $(M + H)^+$, 607 $(M + Na)^+$, 629 $(M - H + 2Na)^+$.

Synthesis of G2-macro. Here, 0.14 g (1.1 mmol) of 2-hydroxyethyl methacrylate (HEMA) and 0.20 g (2.0 mmol) of triethylamine (TEA) were dissolved in 6 mL of anhydrous THF. Then a THF solution of 0.27 g (1.3 mmol) of 4-nitrophenyl chloroformate was added in an ice bath. After the solution was stirred at room temperature for 48 h, the produced white salt TEA·HCl was filtrated, and the filtrate was collected and evaporated in vacuo. The middle product 2-((4-nitrophenoxy)carbonyloxy)-ethyl methacrylate (**1**, Scheme 1) was used without further purification. Then, a dichloromethane solution of **1** was added dropwise to an ice-cooled, stirred solution of 0.56 g (0.50 mmol) **DG2** and 0.40 g (4.0 mmol) TEA in dry CH_2Cl_2 (15 mL). The mixture was stirred at room temperature for 48 h and the solvent was evaporated in vacuo. The crude product was purified by dissolution−precipitation repeatedly from methanol/diethyl ether (1/20) to afford the monomer **G2-macro** as a light yellow solid with 51.7% yield (0.32 g). The structure and molecular weight of the monomer were determined by ^{1}H NMR, ^{13}C NMR, FTIR, and ESI MS.

G2-macro. This was obtained as a light yellow solid. Yield: 51.7%. ^{1}H NMR (300 MHz, DMSO-d_6, TMS, T = 298 K): 8.10−7.45 (br, 10H, CON*H*), 7.04 (br, 1H, OCON*H*), 6.02 (s, 1H, C*H*$_2$=C), 5.68 (t, 1H, C*H*$_2$=C), 4.40−4.06 (m, 4H, OC*H*$_2$C*H*$_2$O), 3.20−2.98 (m, 20H, NHC*H*$_2$C*H*$_2$NH (16H) and C*H*$_2$CH$_2$N (4H)), 2.98−2.90 (br, 2H, C*H*$_2$CH$_2$N (focal)), 2.65 (br, 12H, C*H*$_2$CH$_2$CO), 2.44 (br, 6H, CH$_2$C*H*$_2$N), 2.20 (br, 12H, CH$_2$-C*H*$_2$CO), 2.03−1.93 (t, 8H, C*H*$_2$CH$_2$CH$_3$), 1.85 (s, 3H, CH$_2$=C(C*H*$_3$)), 1.60−1.35 (m, 8H, CH$_2$C*H*$_2$CH$_3$), 0.84−0.78 (t, 12H, CH$_2$CH$_2$C*H*$_3$). ^{13}C NMR (75 MHz, DMSO-d_6, TMS, T = 298 K): 172.19, 171.46, 171.17, 166.40, 155.94, 135.66, 125.93, 63.03, 61.66, 52.10, 49.52, 38.40, 38.27, 37.37, 36.77, 33.07, 18.58, 17.88, 13.57. FTIR (KBr, cm^{-1}): 3522 (br), 3175, 3088, 2966, 2876, 1714, 1648, 1545, 1451, 1378, 1251, 1140, 1034, 661. ESI MS: calcd for $C_{55}H_{100}N_{14}O_{14}$, 1181; found, 1182 $(M + H)^+$, 1204 $(M + Na)^+$, 1220 $(M + K)^+$.

Synthesis of PG1-macro. Conventional radical polymerization was performed with 2,2′-azobis(isobutyronitrile) (AIBN) as an initiator in a degassed sealed tube. **G1-macro** (0.40 g, 0.68 mmol), AIBN (1.9 mg, 0.012 mmol), and dry DMF (0.85 mL) were placed in a Schlenk tube. After the solution was thoroughly deoxygenated by three freeze−pump−thaw cycles, the tube was sealed and heated to 60 °C for 24 h. After being cooled to room temperature, the product was purified by dissolution−precipitation twice from methanol/diethyl ether (1/40) and dried under vacuum for 24 h to yield a polymer as a pale yellow powder. Two polymers of the first generation, named as **PG1-macro** (0.35 g, 87.5%) and **PG1-macro2** (0.30 g, 90.0%), were synthesized by using different proportion of AIBN. The detailed polymerization conditions are listed in Table 1, and the structure and molecular weight of the polymers were determined by ^{1}H NMR, FTIR, and GPC.

PG1-macro (***PG1-macro2***). This was obtained as a pale yellow powder. ^{1}H NMR (400 MHz, DMSO-d_6, TMS, T = 298 K): 7.95 (br, CON*H*), 7.82 (br, CON*H*), 6.91 (br, OCON*H*), 4.12 (br, OC*H*$_2$C*H*$_2$O), 3.34 (s, H_2O), 3.09 (br, NHC*H*$_2$C*H*$_2$NH and C*H*$_2$CH$_2$N), 2.65 (m, C*H*$_2$CH$_2$CO), 2.45 (br, CH$_2$C*H*$_2$N), 2.19 (br, CH$_2$C*H*$_2$CO), 2.05−2.01 (t, C*H*$_2$CH$_2$CH$_3$ and C*H*$_2$C(CH$_3$) in the main chain), 1.52−1.47 (m, CH$_2$C*H*$_2$CH$_3$ and C*H*$_2$C-(CH$_3$) in the main chain), 0.85−0.81 (t, CH$_2$CH$_2$C*H*$_3$ and CH$_2$-C(C*H*$_3$) in the main chain). (Note: CH_2 and CH_3 in the main chain were at 0.80−2.30 ppm and they were shielded by the signals of protons in the dendrons on the side chain). FTIR (KBr, cm^{-1}): 3524 (br), 3083, 2963, 2875, 1716, 1650, 1545, 1453, 1379, 1250, 1144, 1032, 966, 673. GPC (DMF as eluent): **PG1-macro**, M_n = 101 K, PDI = 1.63; **PG1-macro2**, M_n = 140 K, PDI = 1.63.

Synthesis of PG2-macro. Conventional radical polymerization was performed with benzoyl peroxide (BPO) as an initiator in a degassed sealed tube. **G2-macro** (0.32 g, 0.27 mmol), BPO (1.3 mg, 0.0055 mmol), and dry methanol (0.46 mL) were placed in a Schlenk tube. After the solution was thoroughly deoxygenated by three freeze−pump−thaw cycles, the tube was sealed and heated to 80 °C for 36 h. After being cooled to room temperature, the product was first purified by dissolution−precipitation twice from methanol/diethyl ether (1/40) and dried under vacuum for 24 h to yield a yellow solid. The unreactive monomers were further removed by dialysis using a dialysis membrane

(M_W = 2000) to afford final product (100 mg, yield: 30.8%). The detailed polymerization conditions are listed in Table 1, and the structure and molecular weight of the polymers were determined by ^{1}H NMR, FTIR, and GPC.

PG2-macro. This was obtained as a light yellow powder. ^{1}H NMR (400 MHz, DMSO-d_6, TMS, T = 298 K): 7.95 (br, CONH), 7.83 (br, CONH), 6.98 (br, OCONH), 4.10 (br, OCH_2CH_2O), 3.34 (s, H_2O), 3.08 (br, $NHCH_2CH_2NH$ and CH_2CH_2N), 2.64 (br, CH_2CH_2CO), 2.42 (br, CH_2CH_2N), 2.18 (br, CH_2CH_2CO), 2.03−2.00 (t, $CH_2CH_2CH_3$ and $CH_2C(CH_3)$ in the main chain), 1.51−1.46 (m, $CH_2CH_2CH_3$ and $CH_2C(CH_3)$ in the main chain), 0.84−0.81 (t, $CH_2CH_2CH_3$ and $CH_2C(CH_3)$ in the main chain). (Note: CH_2 and CH_3 in the main chain were at 0.80−2.30 ppm and they were shielded by the signals of protons in the dendrons on the side chain.) FTIR (KBr, cm^{-1}): 3519 (br), 3260, 3088, 2965, 2878, 1717, 1645, 1546, 1461, 1383, 1252, 1148, 1035, 968, 672. GPC (DMF as eluent): **PG2-macro**, M_n = 86 K, PDI = 1.52.

Results and Discussion

Synthesis and Characterization of the Dendronized Polymers. The synthesis of the first and second generation macromonomers (**G*n*-macro** (n = 1, 2)) and the corresponding dendronized polymers (**PG*n*-macro** (n = 1, 2)) are outlined in Scheme 1. The monomers were prepared via two step reactions, including the formation of an activated carbonate **1** by reacting hydroxyl groups of HEMA with 4-nitrophenyl chloroformate, and then incorporating the dendron through the urethane group. The monomers were characterized by ^{1}H NMR, ^{13}C NMR spectroscopy, and the electrospray ionization mass spectrometer (ESI MS). The results agreed with the proposed structures.

The free radical polymerization of **G1-macro** was carried out in DMF solution at 60 °C with AIBN as an initiator, and the polymers with different molecular weights, named as **PG1-macro** and **PG1-macro2** were obtained with excellent yields (~90%, Table 1). The second generation dendronized polymer **PG2-macro** was prepared in methanol solution at 80 °C using BPO as an initiator with the yield of 30% because of the poor solubility and strong gelation ability of **G2-macro** in DMF. The molar masses of all the polymers were in the range of 80−140 thousand (Table 1 and Figure S2, Supporting Information) determined by GPC with DMF containing 0.05 wt % LiBr as the eluent. These polymers were soluble in DMF, DMSO, methanol, and water but insoluble in other common organic solvents, such as THF, chloroform, acetone, and EtOAc.

The structures of these polymers were evidenced by FTIR spectra. As shown in Figure 1, the characteristic absorbance peak at 1716 cm^{-1} was related to the stretching vibration of C=O of ester groups in the main chain, while the peaks at 1650 and 1545 cm^{-1} corresponded to amide I ($\nu_{C=O}$) and amide II (δ_{N-H}) in the pendent dendrons (Figure 1).

^{1}H NMR measurements were performed to further confirm the structures of all the polymers. Figure 2 shows the ^{1}H NMR spectra of **PG1-macro** (Figure 2a) and **PG2-macro** (Figure 2b), respectively. Because of the shielding effect of the dendrons, the protons of CH_2 and CH_3 at 0.80−2.30 ppm in the main chain were not clearly visible in the spectra. However, the signals of OCH_2CH_2O (HEMA) protons and OCONH (urethane) protons close to the main chain appeared as the broad peaks at 3.70−4.50 ppm and 6.65−7.25 ppm, respectively (Figure 2).

Differential scanning calorimetric (DSC) measurement was performed to study the thermo-properties of the resulting

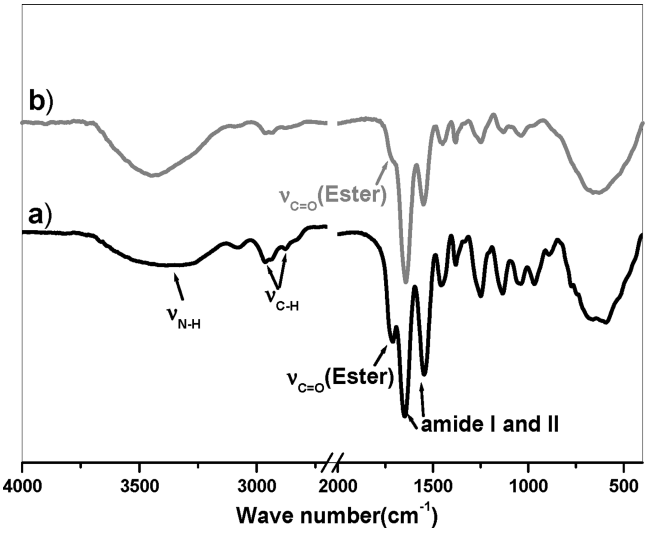

Figure 1. FTIR spectra of (a) **PG1-macro** and (b) **PG2-macro**.

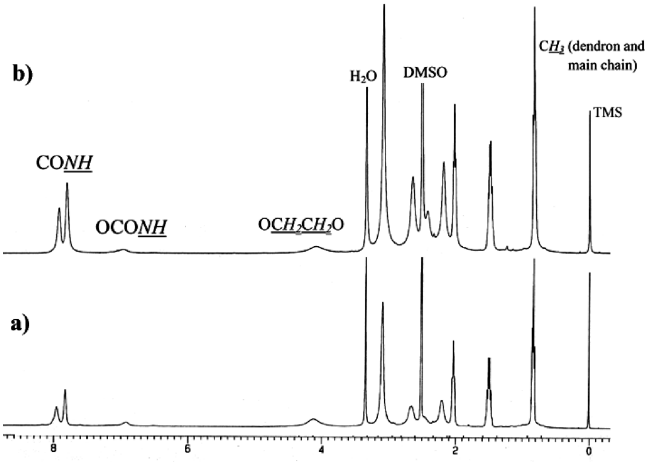

Figure 2. ^{1}H NMR spectra of (a) **PG1-macro** and (b) **PG2-macro** (DMSO-d_6, 298 K).

Table 1. Synthesis and Properties of Dendronized Polymers PG*n*-macro (n = 1, 2)

	polymerization conditions[a]				GPC results[b]				
polymers	[M] (mol/L)	[I]/[M], %	T (°C)	yield (%)	$10^{-5}M_n$	PDI	T_g (°C)[c]	LCST (°C)[d]	pH_{tran}[e]
PG1-macro	0.8	1.7	60	87.5	1.01	1.63	30.7	19.8 (23.8)	6.6
PG1-macro2	0.8	1	60	90.0	1.40	1.63	32.6	15.7 (19.2)	6.5
PG2-macro	0.6	2	80	30.8	0.86	1.52	28.6	27.6 (33.3)	7.8

[a] [M] and [I] represented the concentration of monomer and initiator, respectively; AIBN and DMF were used as the initiator and solvent for **PG1-macro**, and **PG2-macro** was prepared in methanol with BPO as the initiator. [b] All the GPC measurements were done in DMF (0.05 wt % LiBr) as the eluent. [c] The glass transition temperature (T_g) was determined based on the first cooling scan by DSC analysis under nitrogen. [d] All the LCST values were determined by the turbidity measurements with the polymer concentration of 1.0 mg mL^{-1}; The values inside parentheses corresponded to the LCSTs at the polymer concentration of 0.25 mg mL^{-1}. [e] The pH_{tran} was defined as the pH at which the transmittance at λ = 550 nm had reached 50% of its initial value (the transmittance at low pH). Through the turbidity measurements, the pH_{tran} values were obtained by determining a series of polymer solutions (0.25 mg mL^{-1}) with different pHs at 25 °C.

dendronized polymers. As shown in Table 1 and Figure 3, during the first cooling run, the polymers showed glass transition temperature (T_g) at 30.7, 32.6, and 28.6 °C for **PG1-macro**, **PG1-macro2**, and **PG2-macro**, respectively. Similar with our previous report,[26] the T_g of **PG*n*-macro** decreased with increasing the generation of dendrons. Such results might be mainly due to the dendritic architecture. The higher generation dendrons attached along the polymer main chain would occupy more room and wrap the polymer chain inside, resulting in the polymers with softer nature from the structure of dendrons and leading to a decrease in T_g. This result was in accordance with that reported by Khan et al.,[28] who found that the T_g of the ethyl cellulose derivatives functionalized with amidoimide dendrons underwent a significant decrease as a result of the substitution by the appendage of amidoimide dendrons, especially the G2 dendron-functionalized polymers showed lower T_g. Additionally, compared with **PG1-macro**, **PG2-macro** showed a noticeable broadening of the glass transition. This result was in accordance with that reported by Schlüter et al.[29] Structurally, the number of branching point will increase with the generation increasing, which would locally reduce the segmental mobility responsible for the glass transition. Additionally, increasing the generation also involves an increase of the number of end groups, causing the increase of the segmental mobility. As a result, segmental relaxation times would become broader, and consequently contributed to a broadening of the transition. Moreover, **PG1-macro2** (M_n = 140 K) exhibited a slightly higher T_g than **PG1-macro** (M_n = 101 K) for the higher molecular weight of the former. This is reasonable because, generally, the transition temperature relates closely with the degree of polymerization (DP). If the intra- and inter- molecular interactions or the conformation of the polymer does not change significantly with DP, the T_g will shift to higher temperatures as the DP increases.

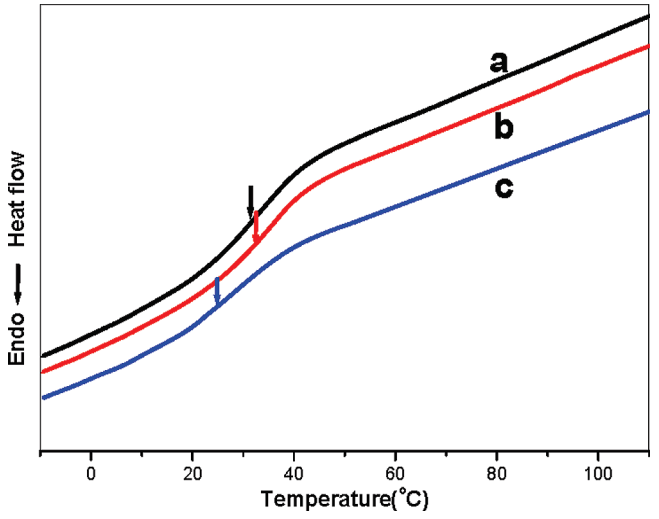

Figure 3. DSC thermograms of **PG*n*-macro** (n = 1, 2) polymers based on the first cooling scan at a cooling rate of 10.0 °C/min under nitrogen atmosphere. In the figure, the black (a), red (b), and blue (c) curves represent **PG1-macro**, **PG1-macro2**, and **PG2-macro**, respectively.

Thermo-Responsive Behavior of PG*n*-macro (n = 1, 2). All the obtained dendronized polymers were water-soluble at low temperatures. The transparent solutions turned turbid with temperature increasing, and became clear again as the temperature decreased, indicating the occurrence of phase transitions and the reversible thermo-responsiveness. UV−vis spectroscopy was used to measure the transmittance of the solution (λ = 550 nm) as a function of temperature in order to determine the LCSTs of **PG*n*-macro** (n = 1, 2). Figure 4a shows the transmittance change of **PG1-macro** and **PG2-macro** at 1.0 mg mL^{-1} in 10 mM phosphate buffered solution (pH = 7.4). Both of them showed relative sharp transition with the LCSTs of 19.8 °C for **PG1-macro** and 27.6 °C for **PG2-macro**, demonstrating the dependence of LCSTs on the generation of dendrons, which was in correspondence with the report by Zhang et al.[22] The reasonable explanations may involve the balance of hydrophilicity and hydrophobicity in the polymer structures varied with pendent dendrons. It is well-known that the ratio of the hydrophobic and hydrophilic units in a polymer chain is crucial to the alternation of LCST. In general, hydrophilic segments shift LCST to a higher temperature,[30] and hydrophobic units show the tendency to decrease LCST.[31] For the **PG1-macro** and **PG2-macro**, the pendent G1 and G2 dendrons afforded them with different hydrophilic and hydrophobic compositions. The G2 dendron possessed more amide moieties that could strongly interact with adjacent water molecules through hydrogen bonds, which enhanced the hydrophilicity of **PG2-macro** and conduced to a higher LCST. Moreover, as shown in the inset of Figure 4a, the hysteresis was small for **PG1-macro** during one heating and cooling cycle. The same phenomenon was also observed for **PG2-macro** at the same condition (Figure S3, Supporting Information). The small hysteresis might be induced by the hydrogen bonding from the structure of the polymers. Such result is consistent with that reported for a series of first and second generation dendronized polymers by Zhang et al.[22,23]

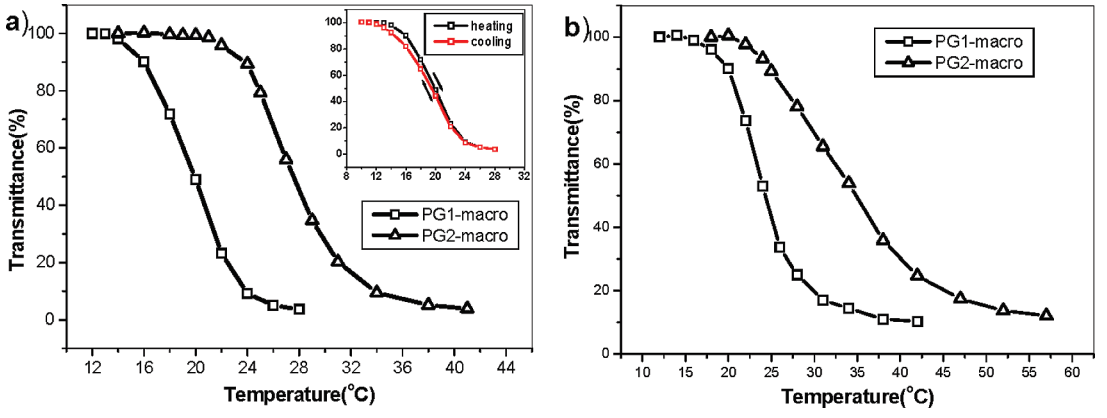

Figure 4. Temperature dependence of the transmittance of (a) 1.0 mg mL^{-1} and (b) 0.25 mg mL^{-1} of **PG1-macro** (□), and **PG2-macro** (Δ) in 10 mM phosphate buffered solution (pH = 7.4). Inset of Figure 4a: the plots of transmittance vs temperature for 1.0 mg mL^{-1} solution of **PG1-macro** (pH = 7.4) during one heating and cooling cycle.

For the most studied linear thermo-responsive polymer, poly(*N*-isopropylacrylamide), the LCST changed only insignificantly with molar masses, for example, the PNIPAM with the molar masses of 5400 and 1600000 showed only ~2 °C deviation in their LCSTs.[32] Interestingly, Kono et al.[16] reported the LCSTs of the globular structure molecules, PAMAM or PPI dendrimers with terminal isobutyramide (IBAM) groups, decreased almost linearly with increasing the generation of the corresponding dendrimers, and a 30 °C decrease in the LCST was observed with the molecular weight increasing from ca. 9150 (G3) to 37800 (G5). Such LCST dependence on molecular weight is due to the compact spherical topology of the dendrimers. Chen and co-workers[33] reported the LCSTs of the hyperbranched polyethylenimines (PEI) ended with IBAM groups were much more sensitive to the molecular weight than those of their dendrimer analogues (PPI dendrimer) due to the topological difference in the location of functional end-groups. In our case, the LCSTs of **PG1-macro** also displayed molecular weight dependence. As shown in Figure 5, the LCST of **PG1-macro** in phosphate buffer at pH 7.4 dropped ~4 °C with M_n rising from 101 to 140 K. The particular architecture of the dendronized polymer and the unique location of peripheral butylamide groups were the possible reasons for the moderate decline of LCST.

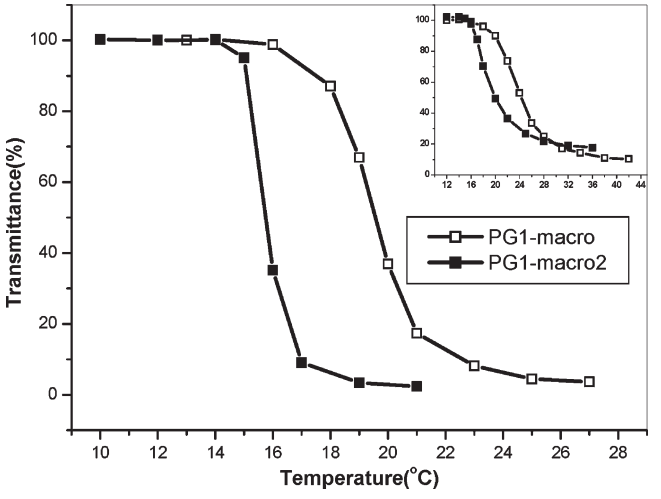

Figure 5. Temperature dependence of the transmittance of 1.0 mg mL^{-1} **PG1-macro** with different molecular weights in 10 mM phosphate buffered solution (pH = 7.4). Inset: plots of transmittance vs temperature for 0.25 mg mL^{-1} **PG1-macro** (□, M_n = 101 K) and **PG1-macro2** (■, M_n = 140 K) in 10 mM phosphate buffer.

Moreover, the LCSTs of these resultant dendronized polymers were also dependent on the concentration. Parts a and b of Figure 4 show the transmittance changes of **PG1-macro** and **PG2-macro** with the concentrations of 1.0 and 0.25 mg mL^{-1} in 10 mM phosphate buffer, respectively. Take **PG1-macro** as an example, the LCST increased from 19.8 to 23.8 °C (Table 1) and the transition zone became broader when the concentration decreased from 1.0 to 0.25 mg mL^{-1}. The similar phenomenon was also observed in our previous report,[26] in which the LCST of **PSADG2** increased from 29.7 to 34.9 °C with the concentration decreasing from 1.0 to 0.1 mg mL^{-1} and the transition temperature region became broader upon dilution.

pH-Responsiveness of PG*n*-macro (*n* = 1, 2). The synthesized **PG1-macro** and **PG2-macro** showed response to the variation of pH for the existence of tertiary amino groups in the interior of pendent dendrons. To demonstrate their pH-responsiveness, a series of polymer solutions with different pHs in 10 mM phosphate buffer were prepared, and the effect of pH on their phase transition behavior was examined. Figure 6a and 6b show the pH dependence of **PG1-macro** and **PG2-macro** on the optical transmittance at 550 nm. Take **PG1-macro** as an example, when pH increased to ca. 6.6, the polymer solution transferred from transparency to opacity because of the aggregation of the polymers, indicating the polymers were more hydrophilic at lower pH and became hydrophobic at higher pH. That was on account of the protonation and deprotonation of tertiary amino groups at different pHs. Furthermore, as shown in Figure 6a, the phase transition of the G1 and G2 dendron-jacketing polymers appeared at pH_{tran} (defined as the pH at which the transmittance reached to 50% of its initial value) of 6.6 and 7.8, respectively. The higher pH_{tran} of **PG2-macro** was attributed to the more hydrophilicity of G2 dendrons. Moreover, the remaining transmittance at elevated pH for the solution of **PG2-macro** at 25 °C was around 70%, suggesting the aggregates were either not so big or not compact, and thus not capable of scattering light efficiently.[34]

Besides the generation, the molecular weight of polymers also showed influence on the pH-responsive behavior. As shown in Figure 6b, the pH_{tran} of **PG1-macro2** (M_n = 140 K) was ca. 6.5 that was slightly lower than that of **PG1-macro** (M_n = 101 K). Additionally, it was also observed that the polymer with higher M_n showed a much sharper transition. The reason is unknown so far, and more samples need to be examined before drawing the conclusions, but more hydrophobicity

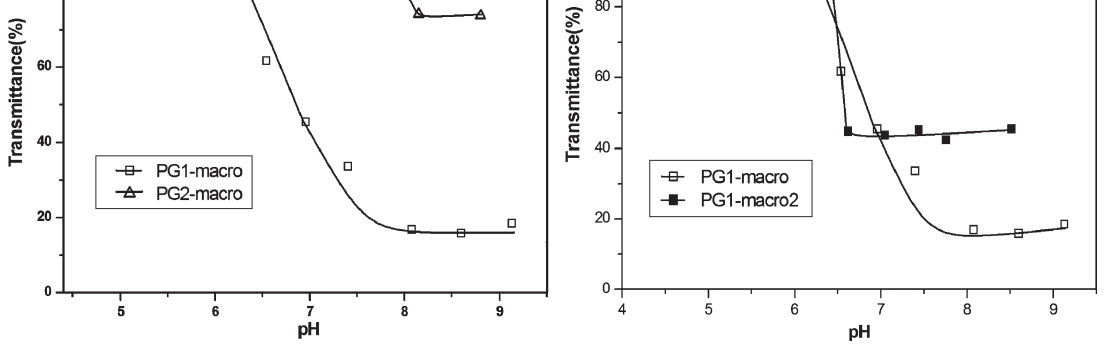

Figure 6. pH dependence of the transmittance at λ = 550 nm of (a) **PG1-macro** (□) and **PG2-macro** (Δ) and (b) **PG1-macro** (□, M_n = 101 K) and **PG1-macro2** (■, M_n = 140 K) at 25 °C in 10 mM phosphate buffered solutions. The concentration of the polymers was 0.25 mg mL^{-1}.

deriving from a much longer main chain of the high molecular weight polymers might be mainly responsible for the results.

Laser Light Scattering Studies. Laser light scattering study of the polymer in dilute solution (0.25 mg mL^{-1}) at different pHs provided a better understanding of the thermally induced phase transition behavior. Figure 7 shows the temperature dependence of the excess scattered intensity of **PG1-macro** solutions at the scattered angle of 90° at pH 5.5 (weak acidicity), 7.0 (neutrality), and 8.6 (weak basicity), respectively. With increasing the temperature, the excess scattered intensity increased for all the solutions at different pHs, yielding the transition temperatures (LCST) of 32, 18, and 12 °C at pHs 5.5, 7.0, and 8.6, respectively (inset of Figure 7). The delayed transition of **PG1-macro** with decreasing pH below 7.0 was due to the protonation of the tertiary amino groups in the interior of dendrons. Under such conditions, the hydrophobic attraction of the peripheral butylamide groups was weakened because of the electrostatic repulsion between the positively charged tertiary amino groups. As a result, a much higher LCST was obtained. On the contrary, the LCST of the polymers decreased slowly at pH above 7.0. Our findings were similar to those reported by Kono et al.,[16] who found that the LCSTs of the peripheral isobutyramide (IBAM) modified PAMAM dendrimers were almost the same at pH above 7.2, but increased greatly upon decreasing pH below 7.2.

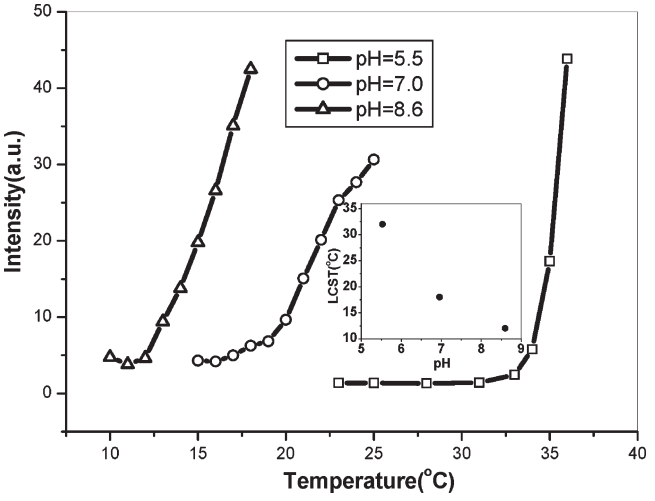

Figure 7. Temperature dependence of the excess scattered intensity of **PG1-macro** at 0.25 mg mL^{-1} in phosphate buffered solutions at pH 5.5 (□), pH 7.0 (○), and pH 8.6 (Δ). The scattered angle is 90°. The inset shows the pH dependence of the LCST of **PG1-macro**.

Figure 8 shows the size distributions of **PG1-macro** at 0.25 mg mL^{-1} with increasing temperature at different pHs. Before the transition points, the solutions were optically clear. However, a bimodal distribution (especially at 30°) was observed at the measured pHs (Figure 8, parts a, a′, and a″). The fast mode with $R_{h,app}$ of about 10 nm was attributed to the separated polymer chains. The size and area ratio of the slow mode were pH dependent. They could be caused either by the incompatibility between the segments[35,36] or by extraordinary behavior of polyelectrolyte (at pH 5.5) in aqueous solutions without enough salt.[37,38] At pH 7.0 and 8.6, the fast mode gradually disappeared with increasing temperature above LCST. Meanwhile, the slow mode increased in size

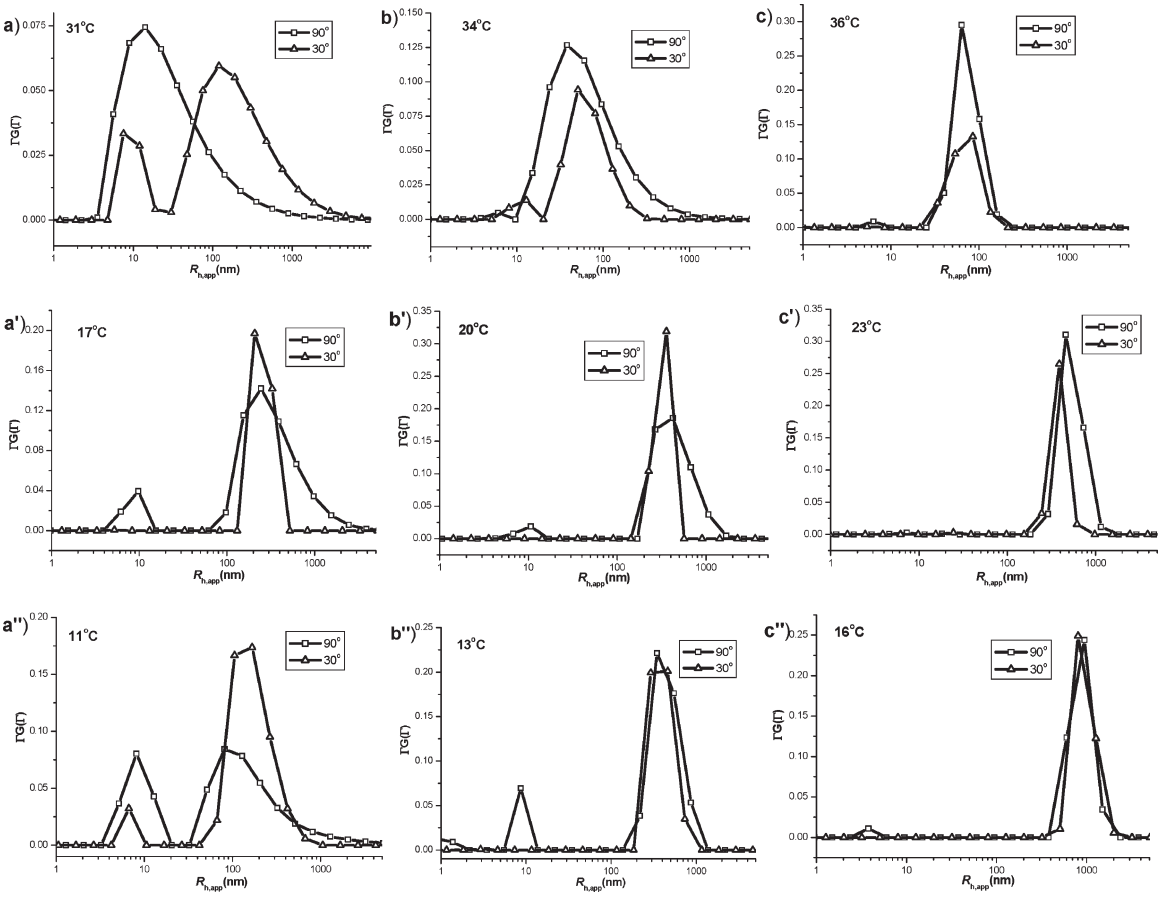

Figure 8. The representative size distribution curves of **PG1-macro** at 0.25 mg mL^{-1} at pH 5.5 (a, b, c), pH 7.0 (a′, b′, c′), and pH 8.6 (a″, b″, c″) during the heating process. The rectangular and triangular symbols denote the data collected at 90° and 30°, respectively.

and area ratio. Eventually, only one narrowly distributed component existed in the system (Figure 8, parts c′ and c″). This was a typical temperature-induced aggregation process. However, this was not the case at pH 5.5, where the size of the slow mode decreased with temperature (Figure 8, parts b and c), indicating that the origin of the slow mode was different from those at elevated pHs.

Figure 9 compares the temperature dependence of the $R_{h,app}$ (measured at 30°) of the slow mode (aggregate) in **PG1-macro** solutions at different pHs. It was obvious that the transition temperature of **PG1-macro** decreased with increasing pH, which was in accordance with the results drawn from the excess scattered intensity (Figure 7). Figure 9 also showed that the change of the aggregate size was highly pH-dependent. The higher the pH, the larger and sharper increase in $R_{h,app}$. At pH 8.6, where **PG1-macro** was not charged at all, the $R_{h,app}$ increased from 150 nm at 10 °C to 950 nm at 16 °C, corresponding to a factor of 6. While at pH 7.0, the size of the aggregates increased from 250 to 375 nm, by a factor of 1.5. At the pH (5.5) where the tertiary amino groups were protonated, a decrease in $R_{h,app}$ was observed. As shown in the inset of Figure 9, the size of the aggregates remained almost no change below 31 °C. A sudden drop in size was observed at the transition point of 32 °C, after which it was maintained at ca. 60 nm with further raising the temperature. Considering that the $R_{h,app}$ of single polymer chain was about 10 nm, thermo-induced aggregation did occur at pH 5.5, as demonstrated by the increase in the excess scattered intensity (Figure 7). The drop in size was due to the unidentified slow mode of charged **PG1-macro**. It was known that the nature of the slow mode of polyelectrolyte in aqueous solution without enough salt was electrostatic,[37,38] while the thermo-induced aggregation was caused mainly by hydrophobic attraction. The different nature of the two driving forces resulted in the abnormal change in size. On the other hand, the size changes in Figure 9 clearly indicated that electrostatic repulsion of the dendrons significantly weakened the degree of aggregation caused by hydrophobic attraction.

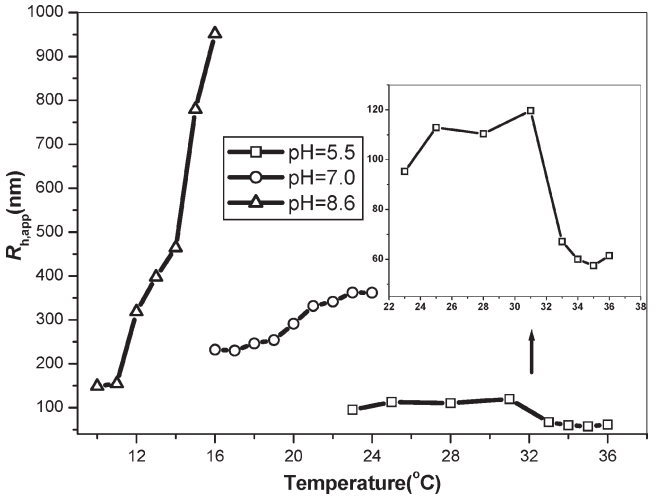

Figure 9. Temperature dependence of $R_{h,app}$ of 0.25 mg mL^{-1} **PG1-macro** at 30° at pH 5.5 (□), pH 7.0 (○), and pH 8.6 (Δ) in phosphate-buffered solutions. The inset magnifies the curve at pH 5.5.

The size distribution of **PG2-macro** was also measured by laser light scattering in a dilute solution (0.25 mg mL^{-1}) at pH 7.4. The results are shown in Figure 10. Compared with the first generation polymer **PG1-macro**, the second generation **PG2-macro** exhibited a much higher LCST at the same conditions (28 °C) (Figure 10a). Moreover, the variation of the size distribution of **PG2-macro** with increasing temperature was similar to that of **PG1-macro**. The area ratio of the fast mode gradually decreased with increasing temperature

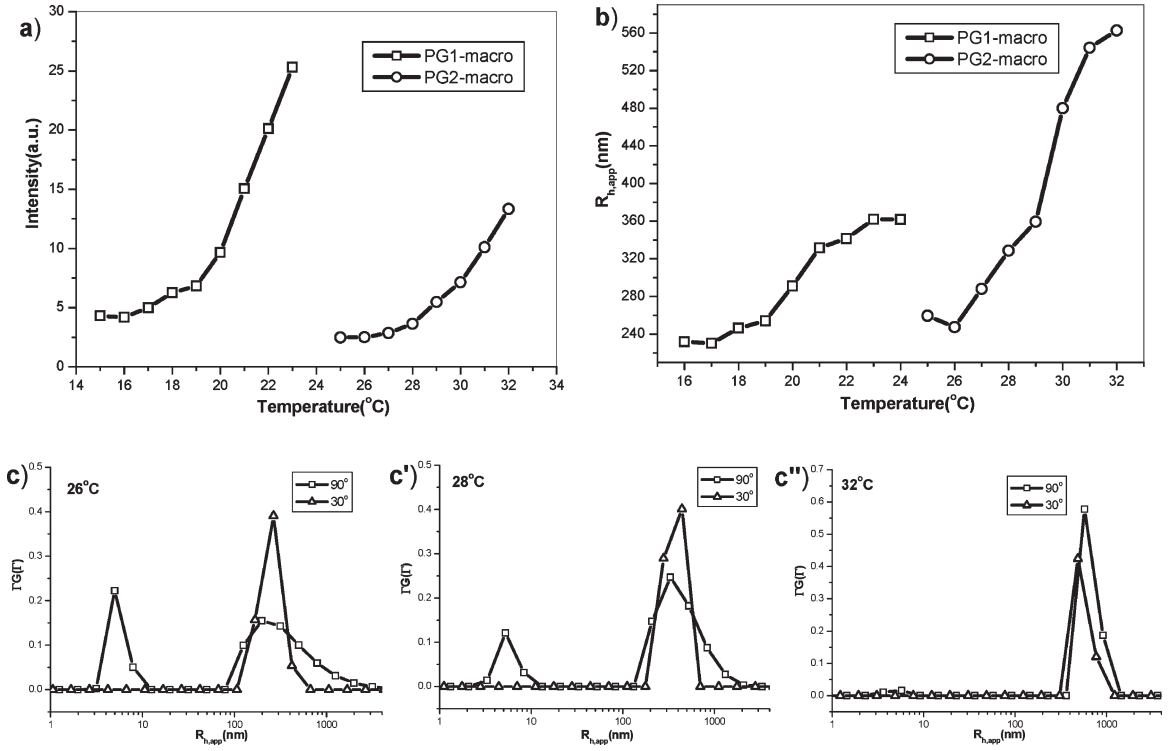

Figure 10. (a) Temperature dependence of the excess scattered intensity of **PG1-macro** (□) and **PG2-macro** (○) at 0.25 mg mL^{-1} in phosphate buffered solutions at pH 7.4. The scattered angle is 90°. (b) Temperature dependence of $R_{h,app}$ of 0.25 mg mL^{-1} **PG1-macro** (□) and **PG2-macro** (○) measured at 30° in phosphate buffered solutions. (c, c′, and c″) The representative size distribution curves of **PG2-macro** at 0.25 mg mL^{-1} at pH 7.4 during the heating process. The rectangular and triangular symbols denote the data collected at 90° and 30°, respectively.

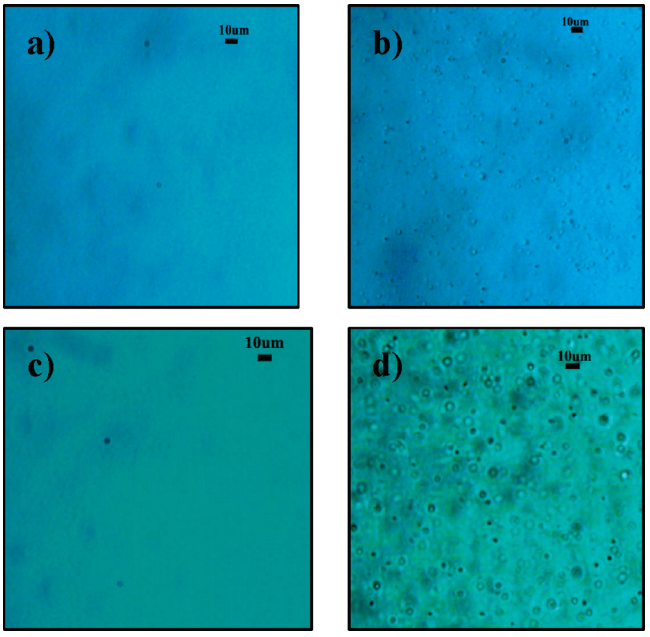

Figure 11. Optical micrographs of **PG1-macro** (a, b) and **PG2-macro** (c, d) in the phosphate buffer at pH 7.4. The temperatures of the solutions maintained at 18 °C (a), 25 °C (b), 20 °C (c), and 36 °C (d), respectively. The concentration of solution is 1.0 mg mL^{-1}.

and totally disappeared at the temperature above LCST. Meanwhile, the size and area ratio of the slow mode increased, and finally only one narrowly distributed component existed in the system (Figure 10, parts c, c′, and c″). However, a larger and sharper increase in $R_{h,app}$ was observed for **PG2-macro**. The $R_{h,app}$ of the aggregates increased from 260 nm at 25 °C to 560 nm at 32 °C, by a factor of 2 (Figure 10b).

Optical Microscopy Studies. Optical microscopy (OM) was used to directly monitor the morphology of the aggregates in polymer solutions. Take **PG2-macro** as a representative, as shown in Figure 11c and d, only a small amount of aggregates was observed in solutions below LCST (20 °C), while more uniform spherical aggregates with the diameter of 3−7 μm appeared as the temperature increased to 36 °C (above LCST), at which the solution turned turbid. It was indicated that the polymer chains spontaneously aggregated together to form the large aggregates when the temperature increased above LCST, which could scatter the light efficiently. Upon cooling, the aggregates disappeared gradually and the solution returned to the original one as the temperature dropped below LCST, suggesting the reversible thermosensitivity of these dendronized polymers (Figure S4, Supporting Information).

Conclusions

A series of dendronized homopolymers (**PG*n*-macro** (n = 1, 2)), with PHEMA as the parent main chain and butylamide terminated poly(amidoamine) dendrons as side chains, were successfully synthesized through the macromonomer route. The molecular weights of the polymers were in the range of 80−140 K determined by GPC with DMF (containing 0.05 wt % LiBr) as the eluent. All the polymers were thermo-responsive and their LCST was dependent on the generation of the dendrons, the concentration of the solutions, and molecular weight of the polymers. It was found that the higher generation dendrons, lower concentration of the solutions, and lower molecular weight of polymers could induce a higher LCST. For the existence of tertiary amino groups in the dendritic units, the polymers also displayed pH-sensitive property. The transition pH value (pH_{tran}) was also dependent on the generation of the pendent dendrons and molecular weight of the polymers. DLS experiments at variable temperature demonstrated that, as the temperature increased, the polymers formed larger aggregates with different $R_{h,app}$ at different pHs through the dehydration and strengthened hydrophobic interactions. In conclusion, the LCST of these new dendronized polymers could be adjusted not only by changing generation of jacketing dendrons and molecular weight of the polymers, but also by altering the concentration and pH of the solutions. Furthermore, the macromonomer route gives dendronized polymers with "perfect" and well-defined structures that could be easily controlled. Such materials may become potential candidates spanning a broad temperature range for drug delivery, sensors, and separation materials etc.

Acknowledgment. This work is financially supported by the National Natural Science Foundation of China (20774003 and 20974004) to X.-R.J.

Supporting Information Available: Figures showing ^{1}H NMR spectrum of **1**, GPC traces for **PG*n*-macro** (n = 1, 2), plots of transmittance vs temperature for **PG2-macro** (pH = 7.4) during one heating and cooling cycle, a series of optical micrographs of **PG2-macro** solution in the process of cooling, and the ESI MS spectra of **G1-macro** and **G2-macro**. This material is available free of charge via the Internet at http://pubs.acs.org.

References and Notes

(1) Yuk, S. H.; Cho, S. H.; Lee, S. H. *Macromolecules* **1997**, *30*, 6856–6859.
(2) Yin, X.; Stöver, H. D. H. *Macromolecules* **2002**, *35*, 10178–10181.
(3) Zhang, X.; Li, J.; Li, W.; Zhang, A. *Biomacromolecules* **2007**, *8*, 3557–3567.
(4) Chang, C.; Wei, H.; Feng, J.; Wang, Z.-C.; Wu, X.-J.; Wu, D.-Q.; Cheng, S.-X.; Zhang, X.-Z.; Zhuo, R.-X. *Macromolecules* **2009**, *42*, 4838–4844.
(5) Roy, D.; Cambre, J. N.; Sumerlin, B. S. *Chem. Commun.* **2009**, 2106–2108.
(6) Mori, H.; Kato, I.; Endo, T. *Macromolecules* **2009**, *42*, 4985–4992.
(7) Ganta, S.; Devalapally, H.; Shahiwala, A.; Amiji, M. *J. Controlled Release* **2008**, *126*, 187–204.
(8) Kumar, A.; Srivastava, A.; Galaev, I. Y.; Mattiasson, B. *Prog. Polym. Sci.* **2007**, *32*, 1205–1237.
(9) Schmaljohann, D. *Adv. Drug Deliver. Rev.* **2006**, *58*, 1655–1670.
(10) Alarcón, C.; de las, H.; Pennadam, S.; Alexander, C. *Chem. Soc. Rev.* **2005**, *34*, 276–285.
(11) Jeong, B.; Gutowska, A. *Trends Biotechnol.* **2002**, *20*, 305–311.
(12) Kikuchi, A.; Okano, T. *Prog. Polym. Sci.* **2002**, *27*, 1165–1193.
(13) Bromberg, L. E.; Ron, E. S. *Adv. Drug Deliver. Rev.* **1998**, *31*, 197–221.
(14) Verdonck, B.; Goethals, E. J.; Prez, F. E. D. *Macromol. Chem. Phys.* **2003**, *204*, 2090–2098.
(15) Gil, E. S.; Hudson, S. M. *Prog. Polym. Sci.* **2004**, *29*, 1173–1222.
(16) Haba, Y.; Harada, A.; Takagishi, T.; Kono, K. *J. Am. Chem. Soc.* **2004**, *126*, 12760–12761.
(17) Haba, Y.; Kojima, C.; Harada, A.; Kono, K. *Angew. Chem., Int. Ed.* **2007**, *46*, 234–237.
(18) Rosen, B. M.; Wilson, C. J.; Wilson, D. A.; Peterca, M.; Imam, M. R.; Percec, V. *Chem. Rev.* **2009**, *109*, 6275–6540.
(19) Frauenrath, H. *Prog. Polym. Sci.* **2005**, *30*, 325–384.
(20) Liang, C. O.; Helms, B.; Hawker, C. J.; Fréchet, J. M. J. *Chem. Commun.* **2003**, 2524–2525.
(21) Peng, Q.; Xu, J.; Li, M.; Zheng, W. *Macromolecules* **2009**, *42*, 5478–5485.
(22) Li, W.; Zhang, A.; Feldman, K.; Walde, P.; Schlüter, A. D. *Macromolecules* **2008**, *41*, 3659–3667.
(23) Li, W.; Zhang, A.; Schlüter, A. D. *Chem. Commun.* **2008**, 5523–5525.
(24) Bolisetty, S.; Schneider, C.; Polzer, F.; Ballauff, M.; Li, W.; Zhang, A.; Schlüter, A. D. *Macromolecules* **2009**, *42*, 7122–7128.
(25) Li, W.; Wu, D.; Schlüter, A. D.; Zhang, A. *J. Polym. Sci., Part A: Polym. Chem.* **2009**, *47*, 6630–6640.

(26) Gao, M.; Jia, X.; Kuang, G.; Li, Y.; Liang, D.; Wei, Y. *Macromolecules* **2009**, *42*, 4273–4281.
(27) Gao, M.; Kuang, G.-C.; Jia, X.-R.; Li, W.-S.; Li, Y.; Wei, Y. *Tetrahedron Lett*. **2008**, *49*, 6182–6187.
(28) Khan, F. Z.; Shiotsuki, M.; Nishio, Y.; Masuda, T. *Macromolecules* **2007**, *40*, 9293–9303.
(29) Zhang, A.; Okrasa, L.; Pakula, T.; Schlüter, A. D. *J. Am. Chem. Soc*. **2004**, *126*, 6658–6666.
(30) Shibayama, M.; Tanaka, T.; Han, C. C. *J. Chem. Phys*. **1992**, *97*, 6842–6854.
(31) Takei, Y. G.; Aoki, T.; Sanui, K.; Ogata, N.; Okano, T.; Sakurai, Y. *Bioconjugate Chem*. **1993**, *4*, 341–346.
(32) Schild, H. G.; Tirrell, D. A. *J. Phys. Chem*. **1990**, *94*, 4352–4356.
(33) Liu, H.; Chen, Y.; Shen, Z. *J. Polym. Sci., Part A: Polym. Chem*. **2007**, *45*, 1177–1184.
(34) Zhang, X.; Li, J.; Li, W.; Zhang, A. *Biomacromolecules* **2007**, *8*, 3557–3567.
(35) Yan, J.; Ji, W.; Chen, E.; Li, Z.; Liang, D. *Macromolecules* **2008**, *41*, 4908–4913.
(36) Ke, F.; Mo, X.; Yang, R.; Wang, Y.; Liang, D. *Macromolecules* **2009**, *42*, 5339–5344.
(37) Förster, S.; Schmidt, M. *Adv. Polym. Sci*. **1995**, *120*, 51–133.
(38) Zhou, K.; Li, J.; Lu, Y.; Zhang, G.; Xie, Z.; Wu, C. *Macromolecules* **2009**, *42*, 7146–7154.